International Journal of Engineering Research and General Science Volume 2, Issue 4, June-July, 2014
ISSN 2091-2730

Numerical Simulation for Heat Transfer Enchancement in a Triangular Ribbed Channel with Winglet Vortex Generators

[1]Amit Garg, [2]Sunil Dhingra
[1]M.Tech. Scholar, Department of Mechanical Engineering, U.I.E.T, Kurukshetra, India
[2]Assistant. Prof., Department of Mechanical Engineering, U.I.E.T, Kurukshetra, India
E-mail-amit.garg337@gmail.com

Abstract: Counter rotating longitudinal vortices produced by winglet in a channel is known to enhance heat transfer. In the present investigation, numerical simulation are performed to study forced convection heat transfer and friction loss behavior in a triangular ribbed channel with longitudinal winglet vortex generator for turbulent airflow through constant heat flux. The cross-section of the ribs placed inside the opposite channel walls to create a reverse flow is an isosceles triangle shape. The rib arrangement, is of staggered array, are introduced. Also, two pairs of the WVGs with various attack angles (a) of 60^0, 45^0 and 30^0 are mounted on the test duct entrance to create a longitudinal vortex flow through the test channel. Work are carried out for a rectangular duct of aspect ratio, AR = 10 and height, H = 30 mm with a single rib height, e/H = 0.13 and rib pitch, P/H = 1.33. The flow rate is in terms of Reynolds numbers based on the inlet hydraulic diameter of the channel ranging from 5200 to 22,000. The processes in solving the simulation consist of modeling and meshing the basic geometry using the package ANSYS-CFD. Then the boundary condition will be set before been simulate in Fluent based on the research paper's experimental data. Finally result has been examined in CFD-Post. This work presents a numerically study on the mean Nusselt number, friction factor and thermal enhancement characteristics. The simulation results show a significant effect of the presence of the rib turbulator and the WVGs on the heat transfer rate and friction loss over the smooth wall channel. The values of Nusselts number and friction factor for utilizing both the rib and the WVGs are found to be considerably higher than those for using the rib or the WVGs alone.

Key words: CFD, Heat transfer, Friction factor, rib, Turbulent flow model, winglet, longitudinal vortex generator, swirl flow

INTRODUCTION

Heat transfer enhancement is the process of modifying a heat transfer surface to increase the heat transfer coefficient. In processing plants, air conditioning plants; petrochemical, biomedical and food processing plants serve to heat and cool different types of fluids. Performance of these heat exchangers can be improved by adding protrusion type vortex generators such as fins, ribs, wings, winglets, etc. on the gas side of the core. When longitudinal vortex generators are placed near a heat transfer surface, they increase the heat transfer by transporting fluid from the wall into the free stream and vice versa. The effectiveness of a vortex generator in enhancing the heat transfer depends on the vortex strength generated per unit area of the vortex generator. Winglets pair kept at an angle of attack is very effective as the longitudinal vortices generated by it persist for hundreds of wing chords downstream of the winglets serve for heat enhancement.

In the past decades, many researchers have investigated the effect of fins, ribs, wings, winglets on heat transfer and friction factor values for a smooth channel in both experimental and numerical studies. Han et al. [1] studied experimentally the heat transfer in a square channel with ribs on two walls for nine different rib configurations for P/e = 10 and e/H = 0.0625. They found that the angled ribs and 'V' ribs yield higher heat transfer enhancement than the continuous ribs and the heat transfer rate and the friction factor were highest for the 60^0 orientation amongst the angled ribs. For heating either only one of the ribbed walls or both of them, or all four channel walls, Han et al. [2] also reported that the former two conditions resulted in an increase in the heat transfer with respect to the latter one. By using a real time Laser Holographic Interferometry to measure the local as well as average heat transfer coefficient, Liou and Hwang [3],[4] investigated experimentally the performance of square, triangular and semi-circular ribs and found that the square ribs give the best heat transfer performance among them. This is contrary to the experimental result of Ahn [5] indicated that the triangular rib performs better than the square one.

Nomenclature

A	convection heat transfer area of channel, m^2	U	mean velocity, m/s
AR	aspect ratio of channel (W/H)	V	volumetric flow rate, m^3/s
Cp	specific heat capacity of air, J/kg K	W	width of channel
D	hydraulic diameter, m(2HW/(H+W))	WVGs	winglet type vortex generators
e	rib height, m		
f	friction factor	Greek letters	
H	channel height, m	α	attack angle of WVGs, degree
h	average heat transfer coefficient, W/m^2 K	ρ	density of air, kg/m^3
k	thermal conductivity of air, W/m K	η	thermal enhancement factor
L	length of tested channel, m	μ	fluid dynamic viscosity, kg s^{-1} m^{-1}
Nu	Nusselt number (hD/k)		
P	pitch (axial length of rib cycle), m	Subscripts	
ΔP	pressure drop, Pa	o	smooth channel
Pr	Prandtl number	conv	convection
Re	Reynolds number (UD/ν)	i	inlet
Q	heat transfer, W	o	out
T_s	Average temperature of heated wall, K	pp	pumping power
T_o	Average temperature of outlet	s	channel surface
T_i	Inlet temperature		
t	thickness of rib, m		

Tanda [6] examined the effect of transverse, angled ribs, discrete, angled discrete ribs, V-shaped, V-shaped broken and parallel broken ribs on heat transfer and friction and reported that 90^0 transverse ribs provided the lowest thermal performance while the 60^0 parallel broken ribs or 60^0 V-shaped broken ribs yielded a higher heat transfer augmentation than the 45^0 parallel broken ribs or 45^0 V-shaped broken ribs. Thianpong et al. [7] again investigated the thermal behaviors of isosceles triangular ribs attached on the two opposite channel walls with AR = 10 and suggested the optimum thermal performance of the staggered ribs could be at about e/H = 0.1 and P/H = 1.0.

In general, the swirl/vortex flow generator is used in augmentative heat transfer in several engineering applications to enhance the rate of the heat and mass transfer equipment such as heat exchanger, vortex combustor, drying process, etc. The best methods of generation of decaying swirl/vortex flow are of winglet classified as delta, triangular and rectangular winglet types [8–15]. These winglets are designed to create longitudinal vortices that help to increase turbulence levels resulting in improved heat transfer performance, albeit with a minimal pressure loss penalty. Heat transfer enhancement by winglet type vortex generators mounted at the leading edge of a flat plate was found to be about 50–60% improvement in average heat transfer over the surface of the plate [9-14].

Biswas et al. [16] carry out numerical and experimental study of flow structure and heat transfer effects of longitudinal vortices in a fully developed channel flow. They define a performance quality factor which indicates heat transfer enhancement for a given pressure loss penalty. Based on the value of this factor, they conclude that the performance of the winglet is best for β of 15^0. Sohankar and Davidson [17] attempt unsteady three-dimensional Direct Numerical Simulation (DNS) and Large Eddy Simulation (LES) of heat and fluid flow in a plate-fin heat exchanger with thick rectangular winglet type vortex generators at Reynolds and Prandtl numbers of 2000 and 0.71, respectively. Pongjet [18] conducted experimental result indicated that the use of the ribs along with the WVGs causes a moderate pressure drop increase, f/f_0=2.2–5.5, especially for the in-line rib array and the larger attack angle, and also provides considerable heat transfer augmentations, Nu/Nu_0=2.2–2.6, depending on the attack angle and Reynolds number values. The combined staggered rib and the WVGs with lower angle of attack should be applied instead of using the rib/WVGs alone to obtain higher heat transfer and performance of about 40–65%, leading to more compact heat exchanger.

In the present study, the effect of swirling flow generating by the winglet vortex generator on heat transfer and pressure drop characteristics in a staggered channel by CFD analysis in ANSYS Fluent 14.0 software. Comparisons of Nusselt number and friction factor with previous correlation [18]. Nusselt number, friction factor and thermal performance factor (η) are examined under uniform wall heat flux using air as testing fluid.

NUMERICAL SIMULATION

2.1 Physical Model. With reference to Fig.2.1.The geometrical details of the flow simulation are: the channel configuration is characterized by the channel height, H and the axial length of cycle or pitch, P, the respective values of which are 30 mm and 40 mm. Each of the ribbed walls 300 mm wide and 440 mm long (L). The rib dimensions are 4 mm high (e) and 20 mm thick (t). Each of the WVGs sheet, 60 mm long and 20 mm high as sketched in Fig.2.2 and placed on the lower plate entrance with the attack angles (α) of 60^0, 45^0 and 30^0 with axial direction. In this work, the combination of the two phenomena, (1) the re-circulating/reverse flow induced by the ribs and (2) the vortex flow created by the WVGs, are supposed to be effective in the vicinity of the tested channel wall, where thermal resistance is high

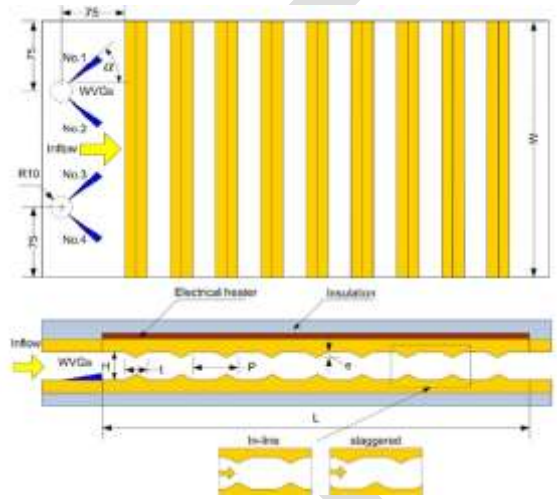

Fig 2.1: Test section with WVGs:

(a) In-line (b) staggered rib

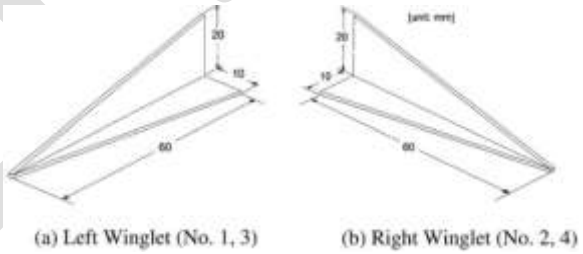

(a) Left Winglet (No. 1, 3) (b) Right Winglet (No. 2, 4)

Fig 2.2: Configuration of WVGs pairs

2.2 Numerical Method. The numerical simulations were carried out using ANSYS-14.0 CFD Software package Fluent-6 version that uses the finite-volume method to solve the governing equations. Geometry was created for air flowing in an electrically heated copper

channel. Meshing has been created in ANSYS model with tetrahedral shapes (Fig.2.3). In this study Reynolds number varies between 5200 to 22000.

Fig 2.3: ANSYS volume-meshing

For turbulent, steady and incompressible air flow with constant properties .We follow the three-dimensional equations of continuity, momentum and energy, in the fluid region.

These equations are below:

Continuity equation:

$$\frac{\partial \rho}{\partial t} + \nabla.(\overline{\rho v}) = 0. \qquad \text{.... (1)}$$

Momentum equation:

$$\frac{\partial(\overline{\rho v})}{\partial t} + \nabla.(\overline{\rho v v}) = -\nabla p + \nabla.(\bar{\tau}) + \rho \bar{g}. \qquad \text{..... (2)}$$

Energy equation:

$$\frac{\partial(\rho E)}{\partial t} + \nabla.(v(\rho E + p)) = \nabla.(k_{eff} \nabla T + (\overline{\tau_{eff}.v})). \qquad \text{.... (3)}$$

Reynolds stress to the mean velocity gradients as shown below:

$$-\rho \overline{u_i' u_j'} = \mu_t \left(\frac{\partial u_i}{\partial x_j} + \frac{\partial u_j}{\partial x_i}\right) - \frac{2}{3}(\rho k + \mu_t \frac{\partial u_k}{\partial x_k})\delta_{ij}.. \qquad \text{... (4)}$$

An appropriate turbulence model is used to compute the turbulent viscosity term μ_t . The turbulent viscosity is given as

$$\mu_t = \rho C \mu \frac{k^2}{\varepsilon}. \qquad \text{.... (5)}$$

Velocity and pressure linkage was solved by SIMPLE algorithm. For validating the accuracy of numerical solutions, the grid independent test has been performed for the physical model.

Table 1.1: Properties of air at 25^0C

Properties	**Value**
Density, ρ	1.225 kg/m^3
Specific heat capacity C_p	1006 J/kg K
Thermal conductivity, k	0.0242 W/m K
Viscosity, μ	1.7894 x10^{-5} kg/m s

Table 1.2: Nodes and Element in geometry are below:

Turbulator	**Nodes**	**Elements**
In-line without WVGs	594336	551250
Staggered without WVGs	654736	607500
WVGs 60^0 staggered rib	270181	1406439
WVGs 45^0 staggered rib	268145	1495412
WVGs 30^0 staggered rib	271617	1495482

Table 1.2 shows that WVGs with staggered ribs have maximum nodes and element in comparison of other turbulators.

In addition, a convergence criterion of 10^{-6} was used for energy and 10^{-3} for the mass conservation of the calculated parameters. The air inlet temperature was specified as 300 K and three assumptions were made in model: (1) the uniform heat flux was along the heated wall. (2) Wall of the inlet calming section was adiabatic. (3) Steady and incompressible flow. In fluent, velocity was taken at inlet section and pressure was taken at outlet section.

2.3 Data Reduction

Three important parameters were considered-friction factor, Nusselt number and thermal performance factor, which determined the friction loss, heat transfer rate and the effectiveness of heat transfer enhancement in the rectangular channel respectively.

The Reynolds number based on the channel hydraulic diameter (D) is given by

$$R_e = \frac{UD}{\nu}$$

The average heat transfer coefficients are evaluated from the measured temperatures and heat inputs. With heat added uniformly to fluid (Q) and the temperature difference of heated wall and fluid (T_s, T_b), average heat transfer coefficient will be evaluated via the following equations:

$$h = \frac{Q}{A\,(T_s - T_b)}$$

in which,

$$T_b = \frac{(T_o + T_i)}{2}$$

The term A is the convective heat transfer area of the heated channel wall. Then, average Nusselt number is written as:

$$Nu = \frac{hD}{k}$$

The friction factor (f) is investigated from pressure drop ΔP across the length of channel (L) using the following equation:

$$f = \frac{2}{(L/D)} \frac{\Delta P}{\rho U^2}$$

RESULTS AND DISCUSSION

3.1 Validation of setup. The CFD numerical result of the smooth channel has been validated with the experimental data as shown in Figures 3.1 and 3.2. These results are within ±9% deviation for heat transfer (Nu) and ±7% for the friction factor (f) with each-other. In low Reynolds number the deviation become small in experimental and CFD results but when Reynolds number become more then these deviation slightly higher in experimental and CFD results, respectively.

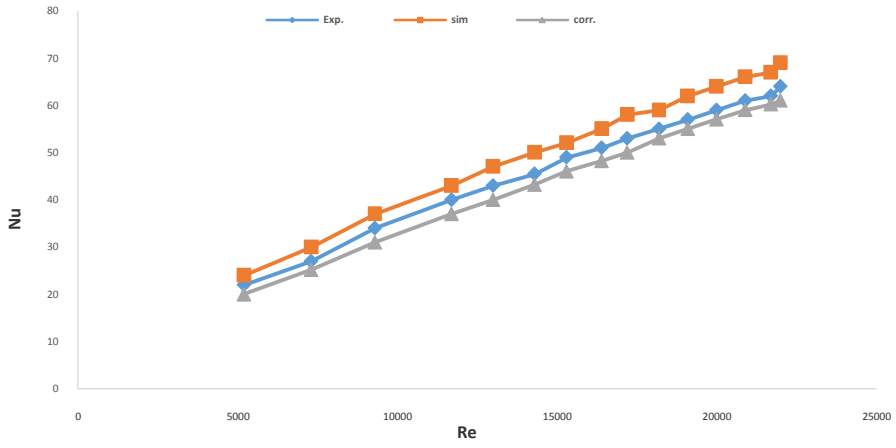

Fig 3.1: Nusselt Vs Reynolds number

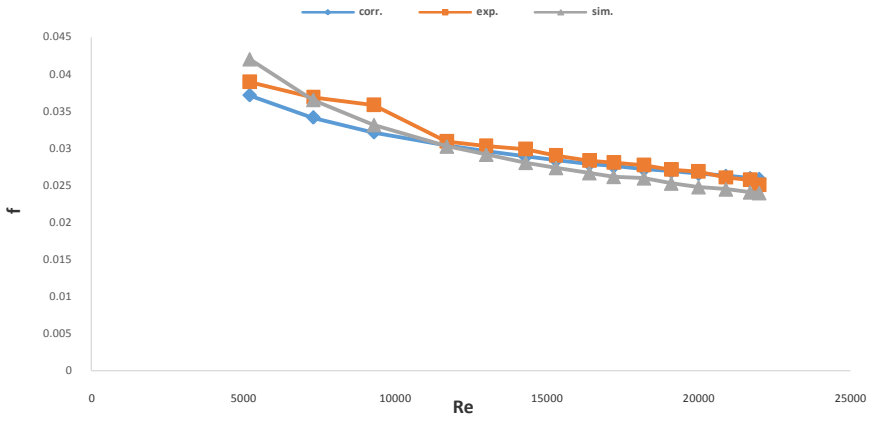

Fig 3.2: Friction factor Vs Reynolds number

3.2 Heat Transfer. Effect of the rib geometry and WVGs on the heat transfer rate is presented in the form of Nusselt number as depicted in Figure-3.3.In the figure, the rib turbulators in conjunction with the WVGs provide considerable heat transfer enhancements in comparison with the smooth channel and the Nusselt number values for using both turbulators increase with the rise of Reynolds number. This is because the ribs interrupt the development of the boundary layer of the fluid flow and create the reverse/recirculating flow behind the rib while the WVGs pairs generate the longitudinal vortex flows that assist to wash up the reverse flow trapped behind the ribs into the core flow. The use of the rib and the WVGs provides a higher heat transfer rate than that of the rib alone at some 40%

The nusselts number with combined staggered and WVGs is 90%, 85% and 80% of the smooth channel for the WVGs with $\alpha=30^0,45^0$ and 60^0 respectively.

The Nusselt number ratio, Nu/Nu_0, defined as a ratio of augmented Nusselt number to Nusselt number of smooth channel plotted against the Reynolds number value is displayed in Fig.3.4. In the figure, the Nusselt number ratio tends to decrease slightly with the rise of Reynolds number for using the combined turbulators. It is interesting to note that at higher Reynolds number, the Nu/Nu_0 values of the in-line and staggered combined turbulators are nearly the same.

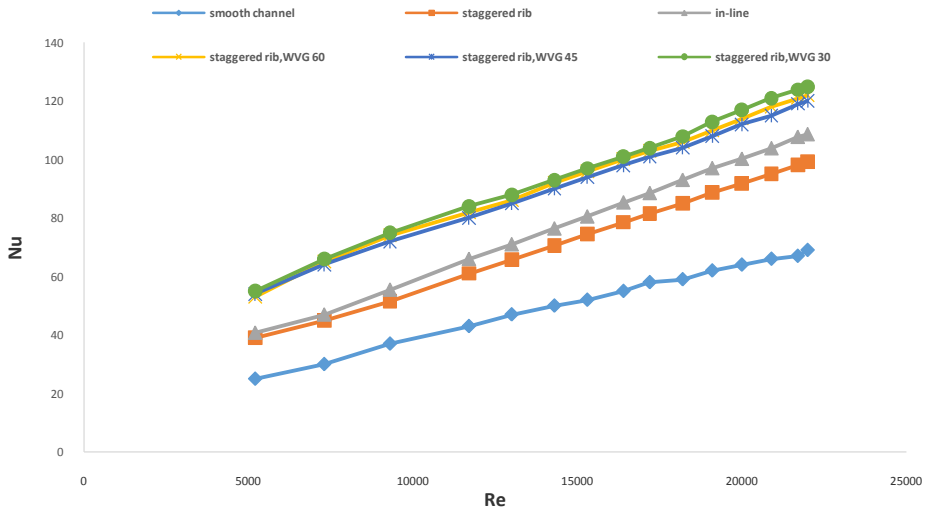

Fig 3.3: Variation of Nu with Re for using ribs & WVGs.

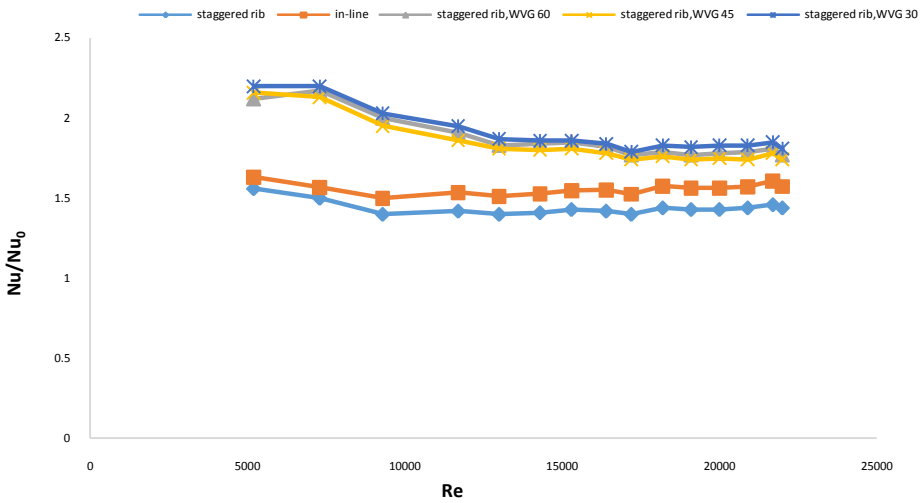

Fig. 3.4: Nu/Nu_o Vs Re for using ribs & WVGs.

3.3 Friction Factor. The variation of the pressure drop is shown in fig.3.5 in terms of friction factor with Reynolds number. In the figure, it is apparent that the use of the combined ribs and WVGs leads to a considerable increase in friction factor over that of the rib alone or the smooth channel. As expected, the friction factor obtained from the combined ribs and WVGs is significantly higher than that from the rib alone, especially for higher the attack angle and the in-line array. The increase in friction factor of the combined rib and WVGs is in a range of 2.3– 5.8 times over the smooth channel, depending on the attack angle, the array and Reynolds number values. The friction factor value of the combined rib and WVGs is found to be higher than that of the rib alone around 25–125%.

Fig. 3.6 presents the variation of the friction factor ratio, f/f_0, with the Reynolds number value. It is observed that the friction factor ratio tends to increase with raising the Reynolds number for all.

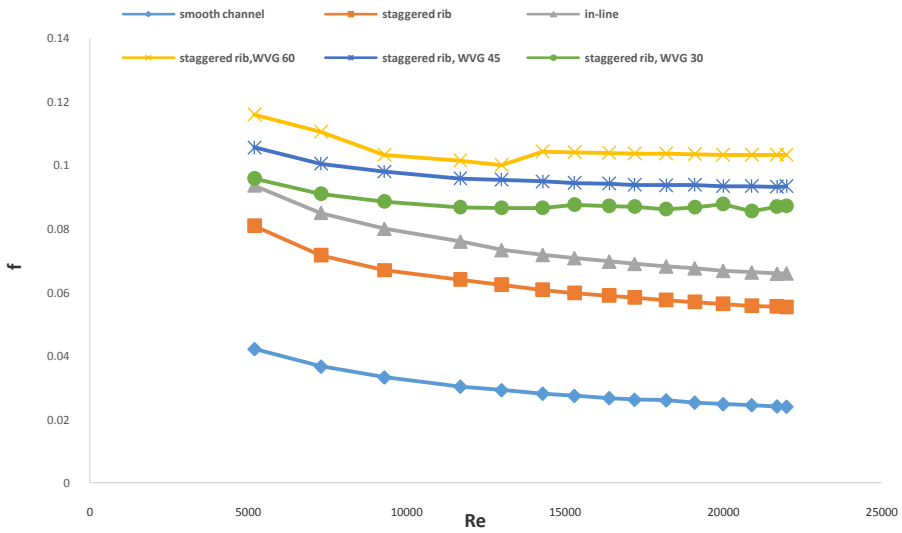

Fig. 3.5: Variation of f with Re for using ribs & WVGs.

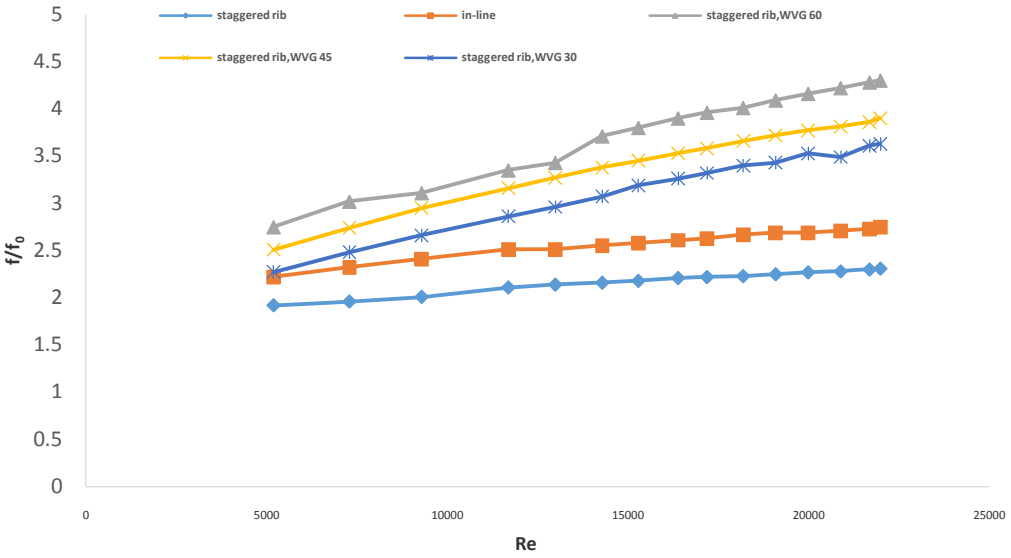

Fig. 3.6: f/f_o Vs Re for using ribs & WVGs.

3.4 Thermal Performance Factor. The variation of the thermal enhancement factor (η) with the Reynolds number values for all turbulators is depicted in Fig. 3.7. For all, the data obtained by measured Nusselt number and friction factor values are compared at an equal pumping power. It is visible in the figure that the enhancement factors (η) for the combined turbulators generally are found to be above unity and to be much higher than those for employing a single use of turbulators. This indicates that the use of ribs in conjunction with the WVGs leads to the advantage over that of a single turbulator. The enhancement factor tends to decrease with the rise of Reynolds number values for all turbulators applied. The 60^0 WVGs yields the enhancement factor lowest among all the WVGs because of the high flow blockage and thus, the larger attack angle of the WVGs should be avoided. The enhancement factor (η) of the combined staggered ribs and 30^0 WVGs is found to be the best among all turbulators used and is about 1.67 is highest at the lowest value of Reynolds number.

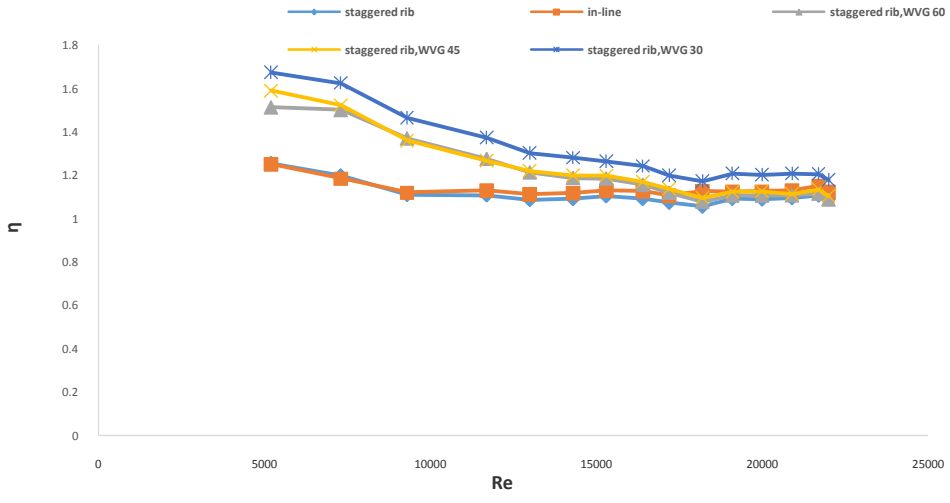

Fig.3.7: Variation of thermal enhancement factor with Reynolds number for various turbulators.

3.5 Velocity and Pressure Contour Plots. In Fig.3.8 velocity contour along the z-y plane shows velocity profile along the WVGs shown that the insertion of the ribs interrupt the development of the boundary layer of the fluid flow and create the reverse/recirculating flow behind the rib while the WVGs pairs generate the longitudinal vortex flows that assist to wash up the reverse flow trapped behind the ribs into the core flow. .Velocity increases due to WVGs and turbulence will be created in channel.

In Fig.3.9 we can see properly that pressure contour shows the pressure drop decreases along the channel length. Due to WVGs pressure drop will also increase because of turbulence in fluid along the WVGs in staggered ribs rectangular channel

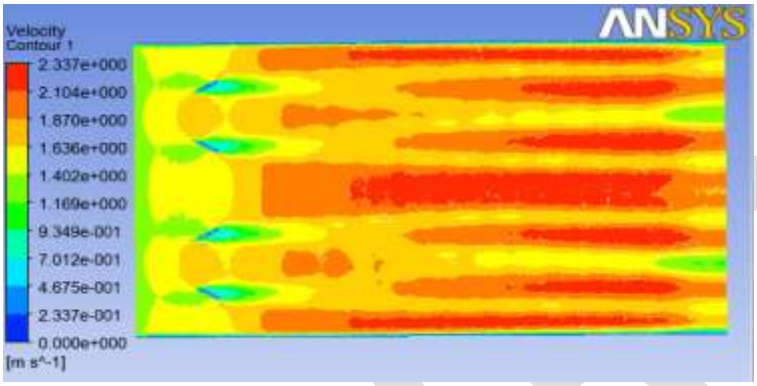

Fig 3.8: Velocity contour along z-y plane

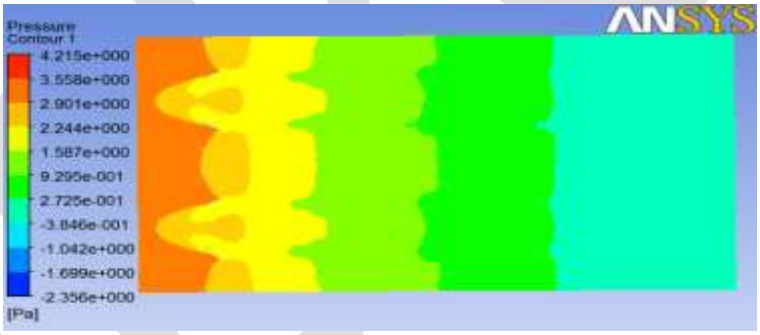

Fig 3.9: Pressure contour along z-y plane

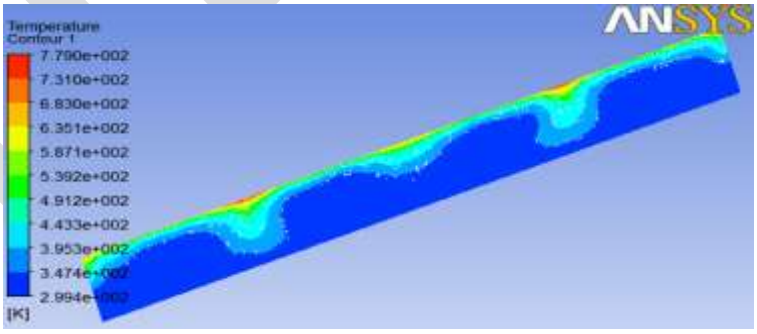

Fig.3.10: Temperature contour along z-x plane

Fig. 3.11(a) & Fig. 3.11(b) shows the velocity contour, and we can find all the values at any point. As we see around the wall and WVGs velocity becomes zero. With the insertion WVGs inside the high aspect ratio channel velocity will be decreased at all Reynolds number compared to that of simple staggered. Fig8. (c), (d) shows the temperature contour, when velocity increases then temperature will be decreases along the flow regime inside channel. Insertion of WVGs causes swirling flow around channel that causes temperature increase in flow. Fig8.(e) (f) shows the pressure contour along the mid plane of rectangular channel. Pressure will increase due to increase of Reynolds number along the length of channel and due to insertion of WVGs pressure will increase due to back flow generated by the wings of vortex pair.

Fig 3.11 Velocity, Temperature and pressure contour at Re No. 5200, 14300, 19100 and 22000 for staggered rib and combined turbulator drawn at Fig. 3.11 (a),(b),(c),(d),(e) and (f)

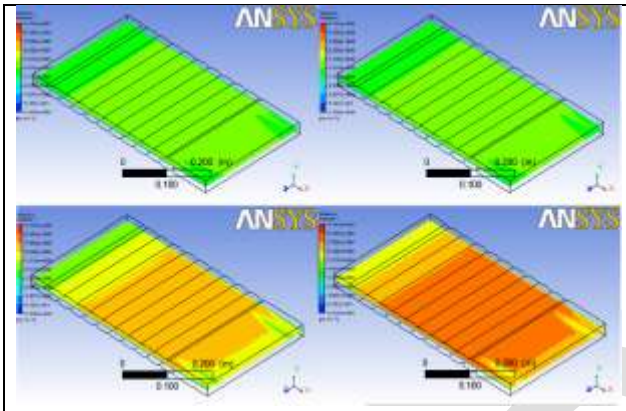

Fig 3.11 (a): Velocity contour for staggered rib

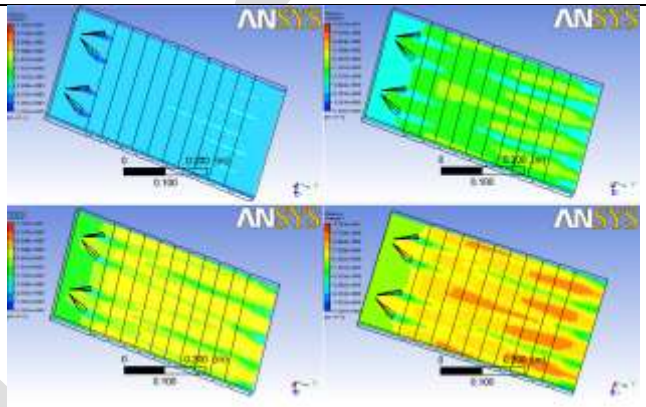

Fig 3.11 (b) velocity contour for combined rib & WVGs

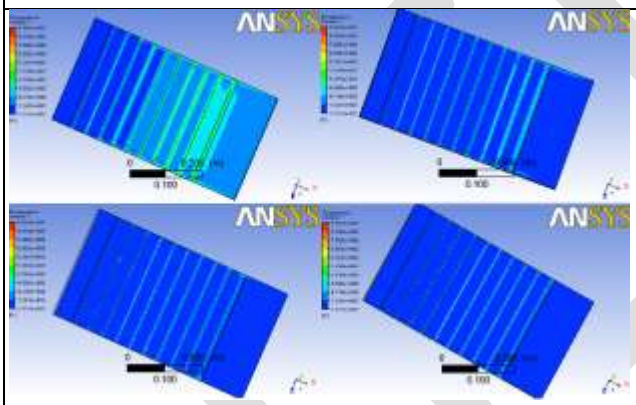

Fig 3.11 (c): Temperature contour for staggered rib

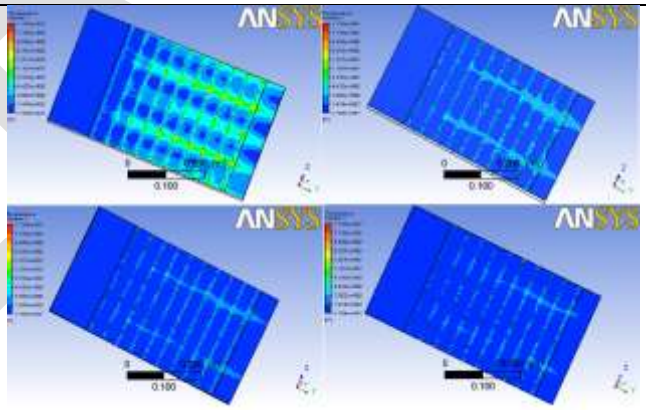

Fig 3.11 (d): Temperature contour for combined rib & WVGs

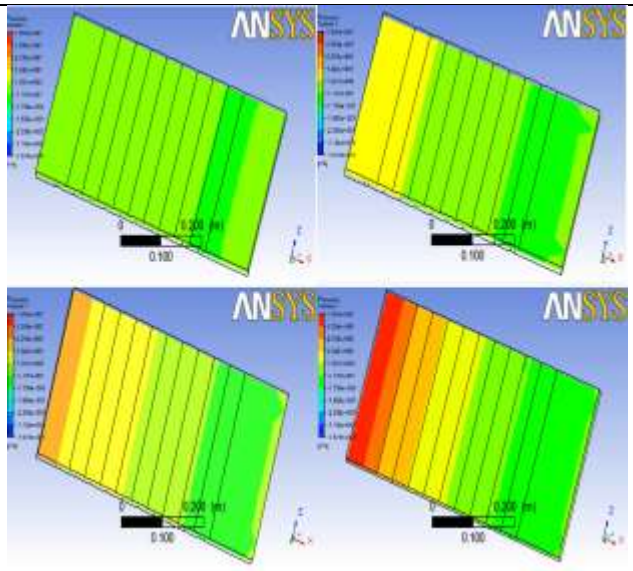

Fig 3.1(e) Pressure contour for staggered rib

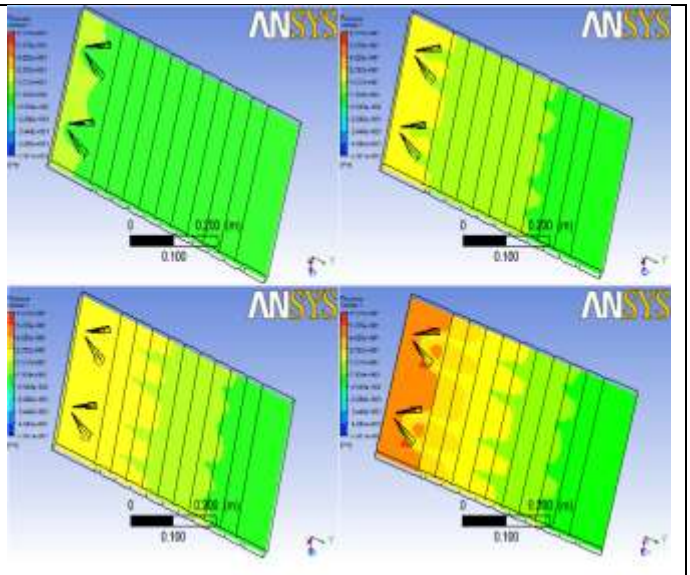

Fig 3.11(f) Pressure contour for combined rib & WVGs

compared to that of simple staggered. At low Reynolds no. the difference is no more but as we go forward there is large difference due to recirculating flow generated by the wings of WVGs

CONCLUSION

The effect of the combined triangular staggered ribs and WVGs turbulators in a high aspect ratio channel for the turbulent regime, Reynolds number varying from 5200–22,000 on the heat transfer (Nu), friction factor (f) and thermal performance factor (η) have been investigated numerically by ANSYS-14 software. The following conclusions are below:

We clearly seen that as the Reynolds number goes on increasing, the heat transfer coefficient also goes on increasing .The combined staggered rib and WVGs for attack angle 30^0, 45^0, and 60^0 heat transfer rate increases 90%, 85%, and 80% more than smooth channel.

The in-line and staggered channel performs lower friction factor values than the combined rib and WVGs. The ratio of friction factor for the combined rib and WVGs with attack angle of 30^0,45^0 and 60^0 are in the range of 2.27-3.63, 2.51-3.9 and 2.75-4.3 respectively.

It has been observed that the thermal performance factor tends to decreases with an increasing attack angle for WVGs and with increases in the Reynolds number. The maximum thermal performance for using combined turbulator WVGs of 30^0,45^0 and 60^0 found to be 1.674, 1.513, and 1.589 respectively.

ACKNOWLEDGEMENTS

The authors gratefully acknowledge the financial support by the Kurukshetra University Research Found.

REFERENCES:

Han JC, Zhang YM, Lee CP. Augmented heat transfer in square channels with parallel, crossed and V-shaped angled ribs. ASME Heat Transfer 1991;113:590 6.

Han JC, Zhang YM, Lee CP. Influence of surface heat flux ratio on heat transfer augmentation in square channels with parallel, crossed, and V-shaped angled ribs. ASME J Turbomach 1992;114:872–80.

Liou TM, Hwang JJ. Turbulent heat transfers augmentation and friction in periodic fully developed channel flows. ASME J Heat Transfer 1992;1145664.

Liou TM, Hwang JJ. Effect of ridge shapes on turbulent heat transfer and friction in a rectangular channel. Int J Heat Mass Transfer 1993;36:931–40.

Ahn SW. The effects of roughness types on friction factors and heat transfer in roughened rectangular duct. Int Commun Heat Mass Transfer 2001;28:933–42.

Tanda G. Heat transfer in rectangular channel with transverse and V-shaped broken ribs. Int J Heat Mass Transfer 2004;47:229–43

Thianpong C,Chompookham T, Skullong S, Promvonge P. Thermal characterization of turbulent flow in a channel with isosceles triangular ribs. Int Commun Heat Mass Transfer 2009;36(7):712–7.

Biswas G, Mitra NK, Fiebig M. Heat transfer enhancement in fin-tube heat exchangers by winglet type vortex generators. Int J Heat Mass Transfer 1994;37:283–91.

Gentry MC, Jacobi AM. Heat transfer enhancement by delta-wing vortex generators on a flat plate: vortex interactions with the boundary layer. ExpTherm Fluid Sci 1997;14:231–42.

Biswas G, Torii K, Fujii D, Nishino K. Numerical and experimental determination of flow structure and heat transfer effects of longitudinal vortices in a channel flow. Int J Heat Mass Transfer 1996;39:3441–51.

Chen Y, Fiebig M, Mitra NK. Heat transfer enhancement of finned oval tubes with staggered punched longitudinal vortex generators. Int J Heat Mass Transfer 2000;43:417–35.

Torii K,Kwak KM, Nishino K. Heat transfer enhancement accompanying pressure-loss reduction with winglet-type vortex generators for fin-tube heat exchangers. Int J Heat Mass Transfer 2002;45:3795–801.

Gentry MC, Jacobi AM. Heat transfer enhancement by delta-wing-generated tip vortices in flat-plate and developing channel flows. ASME J Heat Transfer 2002;124:1158–68.

Kwak KM, Torii K, Nishino K. Simultaneous heat transfer enhancement and pressure loss reduction for finned-tube bundles with the first or two transverse rows of built-in winglets. Exp Therm Fluid Sci. 2005;29:625–32.

Allison CB, Dally BB. Effect of a delta-winglet vortex pair on the performance of a tube-fin heat exchanger. Int J Heat Mass Transfer 2007;50:5065–72.

Biswas, G., Torii, K., Fujii, D., Nishino, K., 1996. Numerical and experimental determination of flow structure and heat transfer effects of longitudinal vortices in a channel flow. International Journal of Heat and Mass Transfer 39, 3441–3451.

Sohankar, A., Davidson, L., 2003. Numerical study of heat and fluid flow in a plate-fin heat exchanger with vortex generators. Turbulence Heat and Mass Transfer 4, 1155–1162.

Promvonge P, Thianpong C, Chompookham T, Kwankaomeng S, 2010.Enhanced heat transfer in a triangular ribbed channel with longitudinal vortex generators. Energy conversion and management 51 (2010) 1242–1249